

Electronic supplementary information (ESI)

**Pinning ultrasmall greigite nanoparticles on graphene for effective  
transition-metal-sulfide supercapacitors in an ionic liquid  
electrolyte†**

Smita Talande,<sup>a,b</sup> Aristides Bakandritsos,<sup>a,c\*</sup> Lukáš Zdražil,<sup>a,d</sup> Petr Jakubec,<sup>a</sup>  
Elmira Mohammadi,<sup>a</sup> Ondřej Tomanec,<sup>a</sup> Michal Otyepka,<sup>a</sup> Volker Presser,<sup>e,f</sup> Radek Zbořil,<sup>a,c,g</sup>  
Jiří Tuček<sup>h,\*</sup>

<sup>a</sup> *Regional Centre of Advanced Technologies and Materials, Faculty of Science, Palacký University,  
Šlechtitelů 27, 783 71, Olomouc, Czech Republic*

<sup>b</sup> *Department of Experimental Physics, Faculty of Science, Palacký University, 17. listopadu 1192/12,  
779 00 Olomouc, Czech Republic*

<sup>c</sup> *Nanotechnology Centre, VŠB–Technical University of Ostrava, 17. listopadu 2172/15, 708 00 Ostrava-  
Poruba, Czech Republic*

<sup>d</sup> *Department of Physical Chemistry, Faculty of Science, Palacký University, 17. listopadu 1192/12, 779  
00 Olomouc, Czech Republic*

<sup>e</sup> *Department of Materials Science & Engineering, Saarland University, Campus D2 2, 66123  
Saarbrücken, Germany*

<sup>f</sup> *INM - Leibniz Institute for New Materials, Campus D2 2, 66123 Saarbrücken, Germany*

<sup>g</sup> *Institute of Organic Chemistry and Biochemistry, Academy of Sciences of the Czech Republic, v.v.i.,  
Flemingovo nám. 2, 16610 Prague 6, Czech Republic*

<sup>h</sup> *Department of Mathematics and Physics, Faculty of Electrical Engineering and Informatics, University  
of Pardubice, náměstí Čs. legií 565, 530 02 Pardubice, Czech Republic*

<sup>\*</sup> *Corresponding authors' e-mail addresses: [a.bakandritsos@upol.cz](mailto:a.bakandritsos@upol.cz); [jiri.tucek@upce.cz](mailto:jiri.tucek@upce.cz)*

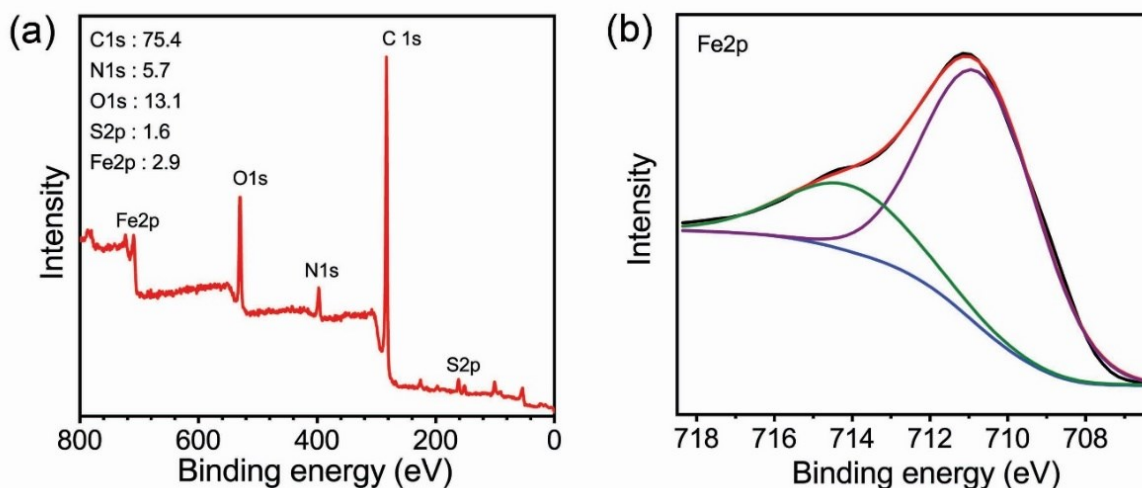


**Figure S1.** (a) X-ray photoelectron emission spectra of GCNFe<sub>3</sub>S<sub>4</sub> hybrid and (b) peak deconvolution for the Fe region before electrochemical testing.

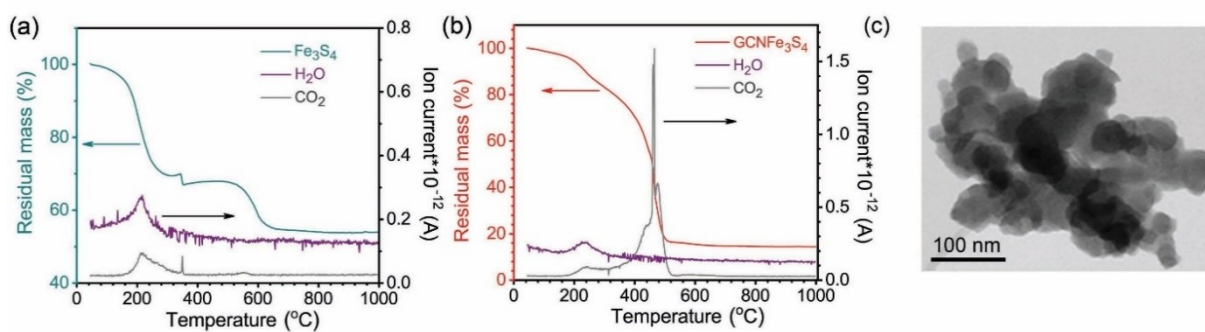


**Figure S2.** (a) Thermogram and (b) evolved gas analysis under air for Fe<sub>3</sub>S<sub>4</sub> and GCNFe<sub>3</sub>S<sub>4</sub> hybrid (c) TEM image of bare Fe<sub>3</sub>S<sub>4</sub>.

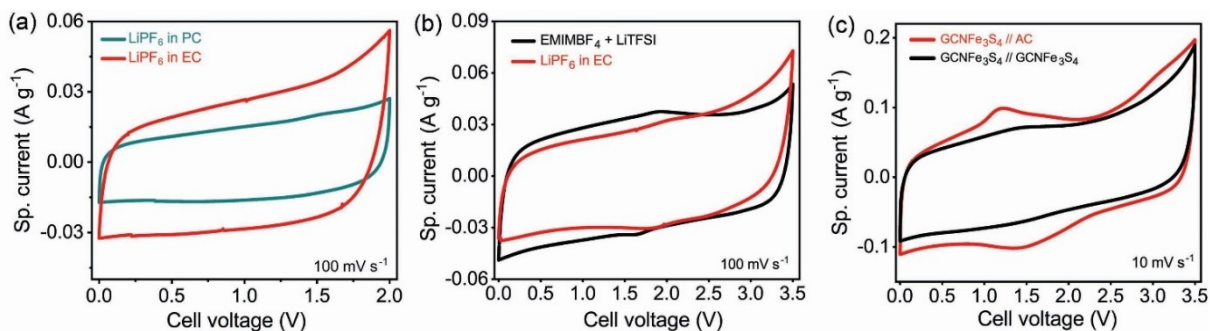


**Figure S3.** (a) Cyclic voltammograms from the GCNFe<sub>3</sub>S<sub>4</sub> symmetric cell in LiPF<sub>6</sub> dissolved in propylene carbonate (PC) and LiPF<sub>6</sub> dissolved in ethylene carbonate (EC) measured at a scan rate of 100 mV·s<sup>-1</sup>. (b) Cyclic voltammograms for GCNFe<sub>3</sub>S<sub>4</sub>//GCNFe<sub>3</sub>S<sub>4</sub> in LiTFSI dissolved in EMIMBF<sub>4</sub> and LiPF<sub>6</sub> dissolved in EC at a scan rate 100 mV·s<sup>-1</sup>. (c) Cyclic voltammograms for asymmetric GCNFe<sub>3</sub>S<sub>4</sub>//AC of total active mass 13 mg and symmetric GCNFe<sub>3</sub>S<sub>4</sub>//GCNFe<sub>3</sub>S<sub>4</sub> of total active mass 4.1 mg in EMIMBF<sub>4</sub> at a scan rate 10 mV·s<sup>-1</sup>.

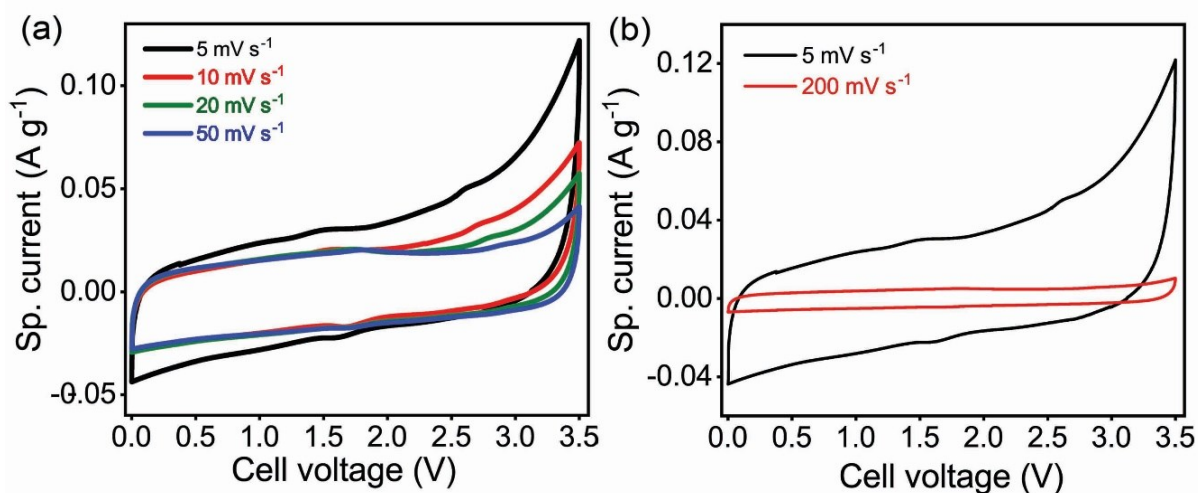


**Figure S4.** (a) Cyclic voltammograms at low scan rates and (b) Cyclic voltammograms normalized to scan rates (low and high), for GCNFe<sub>3</sub>S<sub>4</sub> hybrid using EMIMBF<sub>4</sub>+LiTFSI as an electrolyte in the symmetric cell.

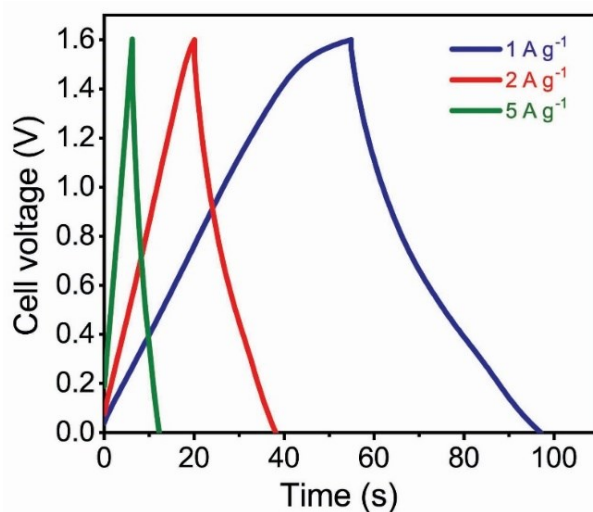


**Figure S5.** Galvanostatic charge/discharge curves at different current densities obtained for GCNFe<sub>3</sub>S<sub>4</sub> hybrid using 6 M KOH as an electrolyte in a symmetric cell.

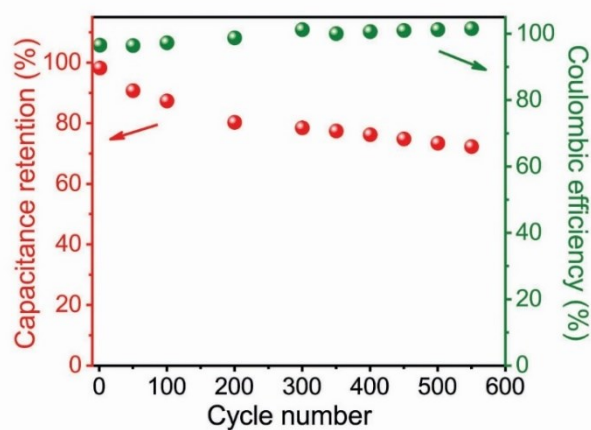


**Figure S6.** Cycling performance of GCNFe<sub>3</sub>S<sub>4</sub> at a specific current of 5 A·g<sup>-1</sup> in an organic electrolyte 1 M LiPF<sub>6</sub> in propylene carbonate.

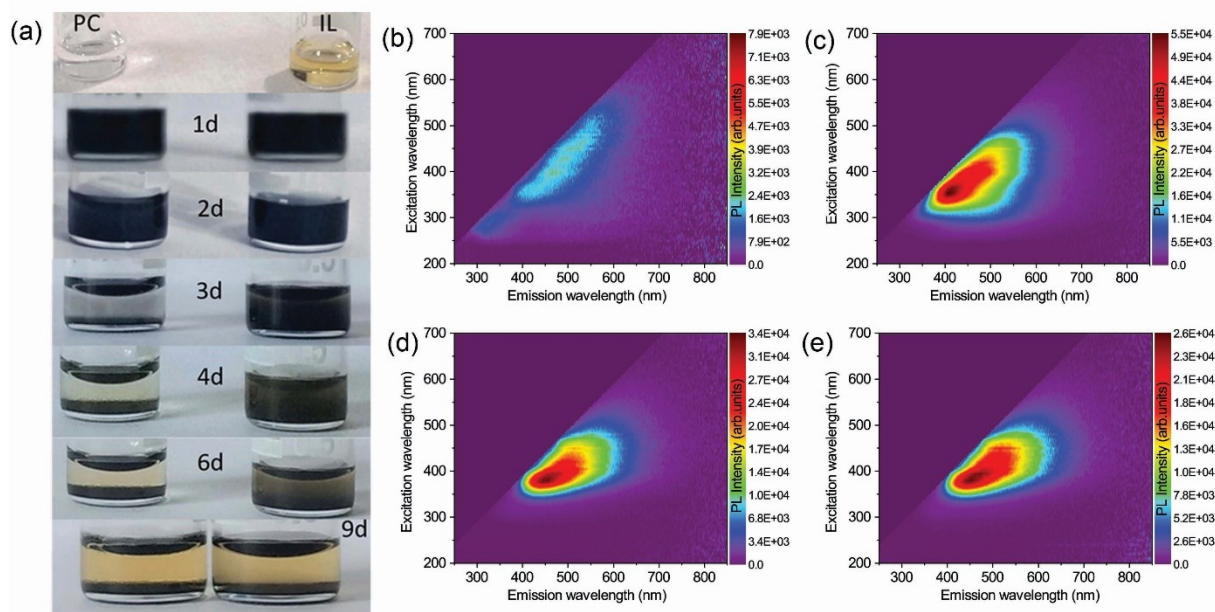


**Figure S7** (a) Photos showing the colloidal stability of GCNFe<sub>3</sub>S<sub>4</sub> material and changes in the color of the two electrolytes: LiPF<sub>6</sub> in propylene carbonate (PC, left) and in the ionic liquid with 1 M LiTFSI (IL, right) in a time-lapse of 9 days. Electrolyte photoluminescence (PL) map of (b) pure LiPF<sub>6</sub> in PC (c) LiPF<sub>6</sub> in PC after 9 d interaction with GCNFe<sub>3</sub>S<sub>4</sub>, (d) pure IL+ LiTFSI, and (e) IL+ Li- salt after 9 d (days) interaction with GCNFe<sub>3</sub>S<sub>4</sub>.

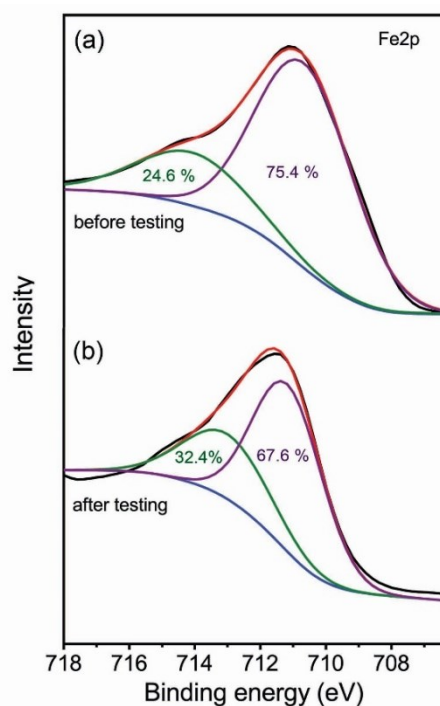


**Figure S8.** X-ray photoelectron emission spectra for the Fe region with deconvoluted components indicating areal% for Fe<sup>3+</sup> and Fe<sup>2+/3+</sup> (a) before and (b) after electrochemical cycling.

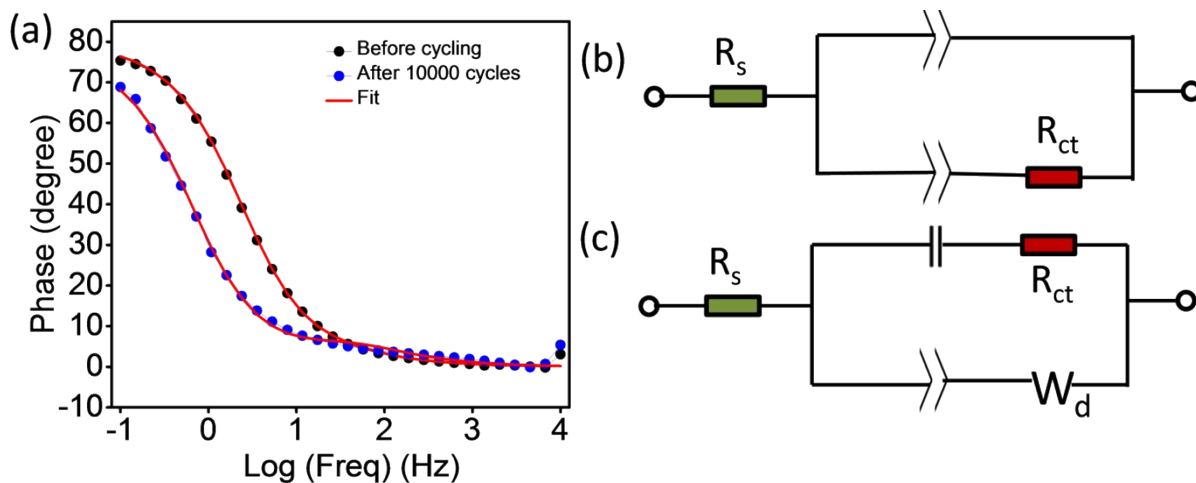


**Figure S9.** (a) Bode plot of GCNFe<sub>3</sub>S<sub>4</sub> before and after electrochemical cycling. (b) Equivalent circuit used for fitting the impedance spectra; before cycling shows source resistance  $R_s = 2.8 \Omega$ , charge transfer resistance  $R_{ct} = 1.6 \Omega$ . (c) The respective equivalent circuit after cycling shows  $R_s = 3.3 \Omega$  and  $R_{ct} = 1.18 \Omega$ .

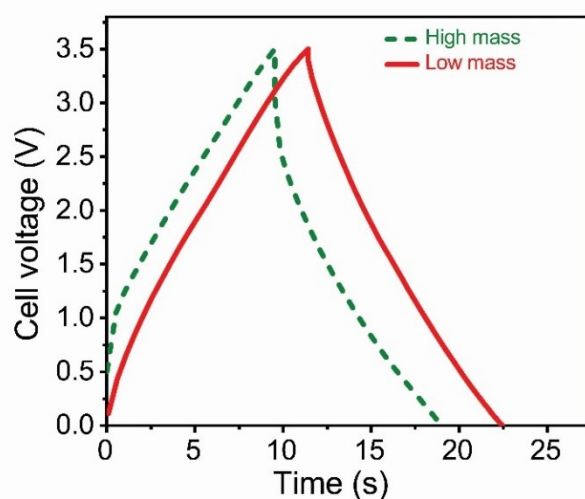


**Figure S10.** Galvanostatic charge/discharge curves for GCNFe<sub>3</sub>S<sub>4</sub> at a specific current of  $5 \text{ A}\cdot\text{g}^{-1}$  for low (total 4.2 mg; that is per area  $0.9 \text{ mg}\cdot\text{cm}^{-2}$ ) and high (total 15.6 mg; that is per area  $3.5 \text{ mg}\cdot\text{cm}^{-2}$ ) electrode mass loadings. For the calculation of the performance, the IR drop was excluded.

**Table S1.** Comparisons of supercapacitors (full-cells only) from literature. The literature-given values appear in black. The recalculated values include the mass of the current collectors (note <sup>i</sup>). [ $\Delta V$ : operating cell-voltage;  $I$ : specific current;  $m$  active material mass;  $m_T$ : total mass (mass of active material + current collectors);  $E$ : specific energy;  $P$ : specific power;  $C$ : capacitance;  $t$ : discharge time; **MW**: microwave; **HT**: hydrothermal. The units are as reported in the header row of the table unless otherwise stated in the specific cells.]

	Anode// Cathode	$\Delta V$ V	Given	Recalculated	Given		Recalculated		C% retention vs $I$	C% retention vs cycling	Electrolyte/ synthesis methods /current collectors/ recalculation details	Ref.
			$I$ A g <sup>-1</sup>	$I$ A g <sup>-1</sup>	$E$ Wh kg <sup>-1</sup>	$P$ kW kg <sup>-1</sup>	$E$ Wh kg <sup>-1</sup>	$P$ kW kg <sup>-1</sup>				
1	AC//Co <sub>9</sub> S <sub>8</sub> - NSA	1.7	-	-	20	0.8	-	-	54% at 10 A g <sup>-1</sup>	84.4% at 1000 <sup>th</sup> cycle	1 M aq. KOH, HT growth on Ni foam (34 mg cm <sup>-2</sup> ). <sup>[ii]</sup>	1
			5	--	8.5	8.2	1.6	0.6			Given $m = 2.8$ mg cm <sup>-2</sup> . From Fig. 6b, $t$ was calculated	
2	AC//Co <sub>9</sub> S <sub>8</sub> @C	1.6	1		58	1	-	-	72% at 18 A g <sup>-1</sup>	86% at 10000 <sup>th</sup> cycle	2 M KOH, multi-step, high temp. treatment, Ni foam	2
			5	0.8	--	--	8	0.6			Given $m = 10//3$ mg cm <sup>-2</sup> . From Fig. 5b, c $t$ was calculated.	
			18	2.8	38	17.2	6.5	2.2				
3	Bi <sub>2</sub> S <sub>3</sub> /S-NCN F//S-NCNF	1.35	8	-	16.4	5.3	-	-	69% at 8 A g <sup>-1</sup>	118% at 2000 <sup>th</sup>	6 M KOH, multi-step synthesis, HT growth on the current collector Counter-el. mass not given	3
4	GCo <sub>0.33</sub> Fe <sub>0.7</sub> S <sub>2</sub> //SG CoNiAl	1.6	-		66.8	0.3	-	-	-	100% at 1000 <sup>th</sup> cycle	3 M KOH, Ni foam, HT synthesis	4
			5	0.3	13	29	1.9	0.3	-	Given $m = 2.5$ mg cm <sup>-2</sup> . From Fig. 8c, $t$ was calculated		
5	FeS <sub>2</sub> //FeS <sub>2</sub>	0.9	1		6.5	0.5	-	-	-	-	3.5 M KOH, Ni foil, HT synthesis	5
			3	0.1	1.5	1.3 <sup>iii</sup>	0.08	0.07	-	-	Given $m = 1.9//1.9$ mg. From Fig. 13b $t$ was calculated	
6	RGO/FeS// Ni(OH) <sub>2</sub>	1.8	0.02 A cm <sup>-2</sup>						-	152% at 1000 <sup>th</sup> cycle	2 M KOH, HT growth on Fe foil (of mass 0.7 mg <sup>iv</sup> )	6
			4.7 A g <sup>-1</sup>	3.4	19.9	4.2	8.1	3	-	-	Given $m=3//1.3$ mg. From Fig. 9b, $t$ was calculated.	

<sup>i</sup> Energy and power values are standardized on the two-electrode metrics, as described in the experimental part.

<sup>ii</sup> A typical value for 80  $\mu$ m thick Ni foam is 34 mg·cm<sup>-2</sup> (as obtained from MTI Corporation, see:

<http://www.mtixtl.com/NickelFoamforBatteryCathodeSubstrate300mmlengthx80mmwidthx0.0.aspx>). Current ( $I$ ) was first calculated from  $C = I \cdot t / m \cdot \Delta V$ , since  $C_m$ ,  $m$ ,  $t$ ,  $\Delta V$  are known. Then, we replaced  $m$  by the total mass of electrode (*i.e.*, active material + Ni foam), to calculate  $C$  for the total electrode mass.

<sup>iii</sup> Calculated  $E$  and  $P$  using Fig. 13b at  $I$  3 A·g<sup>-1</sup> then calculated performance at total electrode mass level.

<sup>iv</sup> Considering Fe density (7.8 g·cm<sup>-3</sup>) and a very thin 1  $\mu$ m Fe foil (Goodfellow, FE000050) mass is obtained (0.7 mg).

7	FeS <sub>2</sub> /GNS//Ni(OH) <sub>2</sub> @C o <sub>9</sub> S <sub>8</sub>	1.7	15	-	27	12.6	-	-	37% at 15 A g <sup>-1</sup> calculated	86% at 5000 <sup>th</sup> cycle	2 M KOH, Ni foam, MW synthesis Solid-state supercapacitor. <sup>[v]</sup>	7
8	rGO <sub>100</sub> <sup>-</sup> CNT <sub>50</sub> <sup>-</sup> Co <sub>3</sub> S <sub>4</sub> //NG	1.6	10	1.17	34.1 <sup>vi</sup> 43.5	8 6.9	3.8	0.9	76% at 10 A g <sup>-1</sup>	90% at 3000 <sup>th</sup> cycle	3M KOH; HT synthesis; Ni foam $m=3 \text{ mg cm}^{-2}$ for 1 <sup>st</sup> el., and mass ratio 0.54, hence mass of 2 <sup>nd</sup> el. =5.55 mg $\text{cm}^{-2}$ . <sup>[vi]</sup>	8
9	NiFeS <sub>2</sub> /3DS G//3DSG	1.6	10	-	31.6	2.2	-	-	70% at 10 A g <sup>-1</sup>	82% at 5000 <sup>th</sup> cycle	6 M KOH; MW synthesis No data given to calculate performance based on $m_T$ .	9
10	Fe-Co- S/NF//rGO	1.6	10	0.6	13.3	5.5	0.8	0.5	62% at 10 A g <sup>-1</sup>	90% at 5000 <sup>th</sup> cycle	1 M KOH, HT growth on Ni foam (2x2 cm <sup>2</sup> ) $m = 2.4/2.1 \text{ mg cm}^{-2}$ . From Fig. 7c, $t$ was calculated	10
11	RGO/ Fe <sub>2</sub> O <sub>3</sub> //CuCo <sub>2</sub> O <sub>4</sub> / CuO	1.6	10	0.36	9.1	8	2.1	1.8	30% at 10 A g <sup>-1</sup>	83% at 5000 <sup>th</sup> cycle	Lower performance; HT growth on Ni foam (2x4 cm <sup>2</sup> ) $t$ was obtained from given $C$ at max. $I = 10 \text{ A g}^{-1}$ . Given $m$ is $7.9 \text{ mg cm}^{-2}$ on +ve electrode. <sup>[vii]</sup>	11
12	Fe <sub>2</sub> O <sub>3</sub> -QDs- 3D GF //3D HPG	1.6	20	1.8	48	16	6.7	2.2	80% at 100 A g <sup>-1</sup>	74% at 12000 <sup>th</sup> cycle	Lower performance, HT synthesis on carbon cloth Given $I$ was based on $m$ only ( $2.0 \text{ mg cm}^{-2}$ ). <sup>[viii]</sup>	12
13	Porous Mn <sub>3</sub> O <sub>4</sub> //Fe <sub>3</sub> O <sub>4</sub>	2	30	3.5	30	30	3.5	3.5	40% at 30 A g <sup>-1</sup>	98% at 30000 <sup>th</sup> cycle	Use of Ni foam and carbon cloth. HT synthesis Given values based on $m$ only ( $2.5 \text{ mg cm}^{-2}$ ) el. area=2 cm <sup>2</sup> and electrode mass ratio is 1:1.5. <sup>[ix]</sup>	13

<sup>v</sup> The TMS are also showed promising energy and power densities for solid state supercapacitors, however, there rate performance needs further improvement as well the improvement on use of low mass current collector is required.

<sup>vi</sup>  $t$  was calculated from the given capacitance value ( $96 \text{ F}\cdot\text{g}^{-1}$ ) at  $10 \text{ A}\cdot\text{g}^{-1}$ ,  $E$  and  $P$  were then recalculated.

<sup>vii</sup> Given values are based on  $m$  only ( $7.6 \text{ mg}\cdot\text{cm}^{-2}$  and  $3.89 \text{ mg}\cdot\text{cm}^{-2}$ ); areal density of Ni foam ( $38 \text{ mg}\cdot\text{cm}^{-2}$ ) and area ( $2 \times 4 \text{ cm}^2$ ) are provided. Hence total mass of Ni foam is 304 mg. Then, we replaced  $m$  by the total mass of electrode (i.e., active material + Ni foam), to calculate  $C_m$  for the total electrode mass.

<sup>viii</sup> Given  $m$  is  $\sim 2.2 \text{ mg}\cdot\text{cm}^{-2}$  per electrode. The area of carbon cloth is  $1.54 \text{ cm}^2$ , considering the mass  $13.5 \text{ mg}\cdot\text{cm}^{-2}$  (as obtained from Fuel cell store, see for instance: <http://www.fuelcellstore.com/fuel-cell-components/gas-diffusion-layers/carbon-cloth/avcarb-1071-hcb> ). The mass of carbon cloth is 20.3 mg per electrode. Using, galvanostatic charge/discharge cycling (Fig. S6), we obtained  $t$ ,  $I$  at  $I_{d,m} 20 \text{ A}\cdot\text{g}^{-1}$ .

<sup>ix</sup> Using reported values for  $I$ ,  $C$  and  $m$ , we calculated  $t$  and then applied current  $I$ . From these values the performance based on  $m_T$  was possible to recalculate considering one electrode with carbon cloth and the other with Ni foam (for mass of carbon cloth and Ni foam see also note [ii])

14	FeOOH//NiMoO <sub>4</sub>	1.7	10	11.3	12.7	4.9	14.4	5.6	67% at 22.5 A g <sup>-1</sup>	80.8% at 10000 <sup>th</sup> cycle	Use of carbon cloth, HT & electrochemical treatment for obtaining the active FeOOH phase, HT growth of NiMoO <sub>4</sub> on Ni foam	14
					7	1.8					Given values are based on full device mass. We recalculated the performance based on $m_T$ . <sup>[x]</sup> Given $m$ is 9 mg·cm <sup>-2</sup> (first row) and 1.6 mg·cm <sup>-2</sup> (second row).	
The FeOOH//NiMoO <sub>4</sub> system was the best performing iron oxide-based supercapacitor among the state-of-the-art, which was identified in the recent publication (Table S3 in the SI file from ref. <sup>15</sup> )												
15	G(CN)ak2//G(CN)ak2	3.5	-	2.9	-	-	5.2	5	-	-	Given values are based on $m_T$	15

<sup>x</sup> The given values correspond to high mass loading (24.5 mg) and reported in Fig. 13b of this reference. Our recalculation was done excluding the mass of the membrane separator (given in the peer review file; response to comment F from reviewer#1).

**Table S2.** Specific energy and power of GCNFe<sub>3</sub>S<sub>4</sub>//GCNFe<sub>3</sub>S<sub>4</sub> cell at different specific currents.<sup>a</sup>

Active mass level	Total electrode mass level	Active mass level		Total electrode mass level		Comments
		<i>E</i>	<i>P</i>	<i>E</i>	<i>P</i>	
<i>I</i>	<i>I</i>	<i>E</i>	<i>P</i>	<i>E</i>	<i>P</i>	
A g <sup>-1</sup>	A g <sup>-1</sup>	Wh kg <sup>-1</sup>	kW kg <sup>-1</sup>	Wh kg <sup>-1</sup>	kW kg <sup>-1</sup>	
1	0.7	37	2	6.3	0.3	Low mass loading of 0.9 mg·cm <sup>-2</sup> (total active mass is 4.2 mg)
2	1.4	35.4	3.5	6.0	0.6	
5	3.4	32.4	8.8	5.5	1.5	
8	5.5	30.3	14.2	5.2	2.4	
10	6.8	29.4	17.7	5.0	3.0	
15	10.2	27.3	26.5	4.7	4.5	
20	13.6	25	35.4	4.3	6.0	
1	0.5	35	2	17.4	0.9	High mass loading of 3.5 mg·cm <sup>-2</sup> (total active mass is 15.6 mg)
		30 μWh·cm <sup>-2</sup>	1.5 mW·cm <sup>-2</sup>			
		49 mWh·cm <sup>-3</sup>	2.4 W·cm <sup>-3</sup>			
2	1.0	30	3	14.9	1.7	
5	2.5	20	8	9.9	3.8	
		28 mWh·cm <sup>-3</sup>	11 W·cm <sup>-3</sup>			
8	4.0	13	11	7.0	5.0	
10	5.0	10	13	5.0	7.0	

<sup>a</sup>To compare the results with other literature reports, where the reported values are calculated using linear equations, we reported the performance values based on the same linear equations, as described in Table S2. Nevertheless, in Table S3, the performance was also reported based on integral equations (see experimental part), for the sake of accuracy.

**Table S3.** Specific energy and power of GCNFe<sub>3</sub>S<sub>4</sub>//GCNFe<sub>3</sub>S<sub>4</sub> cell at different specific currents using equations for non-linear galvanostatic charge-discharge plots.

Active mass level	Total electrode mass level	Active mass level		Total electrode mass level		Comments
<i>I</i>	<i>I</i>	<i>E</i>	<i>P</i>	<i>E</i>	<i>P</i>	
A g <sup>-1</sup>	A g <sup>-1</sup>	Wh kg <sup>-1</sup>	kW kg <sup>-1</sup>	Wh kg <sup>-1</sup>	kW kg <sup>-1</sup>	
1	0.7	31	2	6.6	0.3	Low mass loading of 0.9 mg·cm <sup>-2</sup> (total active mass is 4.2 mg)
2	1.4	29	3	6.3	0.6	
5	3.4	26	7	5.7	1.5	
8	5.5	24	11	5.3	2.5	
10	6.8	23	14	5.0	3.0	
15	10.2	21	20	4.5	4.4	
20	13.6	18	26	4.0	5.7	
1	0.5	30	1.4	14	0.7	High mass loading of 3.5 mg·cm <sup>-2</sup> (total active mass is 15.6 mg)
		41 mWh·cm <sup>-3</sup>	2 W·cm <sup>-3</sup>			
2	1.0	24	2.7	12	1.3	
5	2.5	15	5.6	7	2.8	
5		21 mWh·cm <sup>-3</sup>	8 W·cm <sup>-3</sup>			
	4.0	9	7.5	5	3.8	
10	5.0	6	8.0	3	4.0	

### Supporting References

- 1 X. Han, K. Tao, D. Wang and L. Han, *Nanoscale*, 2018, **10**, 2735–2741.
- 2 S. Sun, J. Luo, Y. Qian, Y. Jin, Y. Liu, Y. Qiu, X. Li, C. Fang, J. Han and Y. Huang, *Adv. Energy Mater.*, 2018, **8**, 1801080.
- 3 W. Zong, F. Lai, G. He, J. Feng, W. Wang, R. Lian, Y.-E. Miao, G.-C. Wang, I. P. Parkin and T. Liu, *Small*, 2018, **14**, 1801562.
- 4 W. Liu, H. Niu, J. Yang, K. Cheng, K. Ye, K. Zhu, G. Wang, D. Cao and J. Yan, *Chem. Mater.*, 2018, **30**, 1055–1068.
- 5 S. Venkateshalu, P. Goban Kumar, P. Kollu, S. K. Jeong and A. N. Grace, *Electrochimica Acta*, 2018, **290**, 378–389.
- 6 C. Zhao, X. Shao, Z. Zhu, C. Zhao and X. Qian, *Electrochimica Acta*, 2017, **246**, 497–506.
- 7 Z. Sun, H. Lin, F. Zhang, X. Yang, H. Jiang, Q. Wang and F. Qu, *J. Mater. Chem. A*, 2018, **6**, 14956–14966.
- 8 A. Mohammadi, N. Arsalani, A. G. Tabrizi, S. E. Moosavifard, Z. Naqshbandi and L. S. Ghadimi, *Chem. Eng. J.*, 2018, **334**, 66–80.
- 9 T. Ma, H. Liu, Y. Wang and M. Zhang, *Electrochimica Acta*, 2019, **309**, 1–10.
- 10 K. Le, M. Gao, W. Liu, J. Liu, Z. Wang, F. Wang, V. Murugadoss, S. Wu, T. Ding and Z. Guo, *Electrochimica Acta*, 2019, **323**, 134826.
- 11 Y. Wang, C. Shen, L. Niu, R. Li, H. Guo, Y. Shi, C. Li, X. Liu and Y. Gong, *J. Mater. Chem. A*, 2016, **4**, 9977–9985.
- 12 Y. Li, H. Zhang, S. Wang, Y. Lin, Y. Chen, Z. Shi, N. Li, W. Wang and Z. Guo, *J. Mater. Chem. A*, 2016, **4**, 11247–11255.
- 13 J. W. Choi, I. W. Ock, K.-H. Kim, H. M. Jeong and J. K. Kang, *Adv. Funct. Mater.*, 2018, **28**, 1803695.
- 14 K. A. Owusu, L. Qu, J. Li, Z. Wang, K. Zhao, C. Yang, K. M. Hercule, C. Lin, C. Shi, Q. Wei, L. Zhou and L. Mai, *Nat. Commun.*, 2017, **8**, 14264.
- 15 S. V. Talande, A. Bakandritsos, P. Jakubec, O. Malina, R. Zbořil and J. Tuček, *Adv. Funct. Mater.*, 2019, **29**, 1906998.